Published in IET Optoelectronics
Received on 24th April 2008
Revised on 14th April 2009
doi: 10.1049/iet-opt.2008.0021

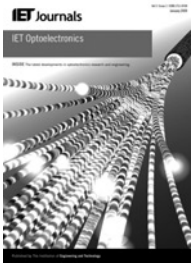

ISSN 1751-8768

Synchronous optical code-division multiple access systems with constant multi-user interference

L.-L. Jau[1] *Y.-H. Lee*[2] *M.-H. Chuang*[2] *C.-L. Yang*[2] *Y.-G. Jan*[2]

[1]*Department of Computer & Communication Engineering, St. John's University, Tamsui, Taipei 25137, Taiwan*
[2]*Department of Electrical Engineering, Tamkang University, Tamsui, Taipei 25137, Taiwan*
E-mail: 691350101@s91.tku.edu.tw

Abstract: A synchronous optical code-division multiple access system with balanced encoder instead of on-off-keying (OOK) encoder is proposed. In the system, the multi-user interference is maintained constant during a frame, and the receiver estimates the interference frame by frame instead of bit by bit. The data rate of the proposed system is no longer severely limited by the electronic processing time in estimating the interference, and the structure of the proposed receiver is simpler than those in OOK systems. In the receiver, both linear and non-linear threshold estimators are introduced. Numerical results show that the proposed system has smaller bit error rate than OOK systems, especially when the number of training bits is increased.

1 Introduction

The code-division multiple access was originally investigated in radio frequency communication systems. In fibre optic communication systems, the bandwidth of the optic fibre is much wider than that of electronic data. To exploit the huge bandwidth of the optic fibre, the optical code-division multiple access (OCDMA) system is a viable alternative for the broadband networks [1–4].

For incoherent OCDMA systems, which are much simpler than coherent systems, the non-negative nature of optical signal has restricted the spreading codes to pseudo-orthogonal unipolar sequences [1, 2, 5–9]. Among them, some are designed for asynchronous OCDMA networks where the users have independent clocks, and others are for synchronous networks. Although the synchronous OCDMA networks need more complex structure to reach the synchronization [10, 11], they have much larger code size, which is defined as the number of available codes, and they allow more simultaneous users [6, 8].

Since the cross-correlations of the unipolar codes are non-negative, the multi-user interference (MUI) increases with the number of simultaneous users. Most of OCDMA systems use the on-off-keying (OOK) scheme in the transmitters to reduce the MUI; that is, only the binary bit-1 is encoded by a signature code sequence. In the receiver, there have also been many schemes proposed and analysed to reduce the error probability resulted from the MUI. For example, optical hardlimiters were utilised in [12–16], error control codes were applied in [17, 18], receivers with interference estimators were proposed in [8, 15, 19], and so on. Among them, it had been shown that receivers with interference estimators have excellent performance since they cancel the interference according to the dynamically estimation of interference.

For the synchronous OOK–OCDMA system using modified prime code (MPC), the structure of the receiver with interference estimator is shown in Fig. 1 [19]. The received power is split into two branches. The upper branch estimates the MUI and tunes the threshold device and then the lower branch detects the received data. For a prime number p, there are p groups of MPCs [6], and each group contains p MPCs. For example, the nine MPCs for $p = 3$ are shown in Table 1. Let $C_{i,j}$ be the jth MPC in the ith group. The synchronous cross-correlation of any

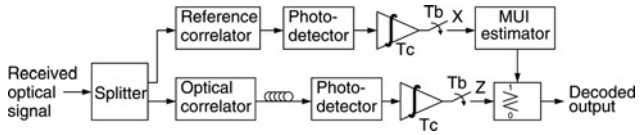

Figure 1 *Parallel structure of OCDMA decoder with interference estimator*

two distinct MPCs can be written as

$$\mathrm{Cr}(\boldsymbol{C}_{i_1,j_1}, \boldsymbol{C}_{i_2,j_2}) = \begin{cases} 0 & \text{for } i_1 = i_2 \text{ and } j_1 \neq j_2 \\ 1 & \text{for } i_1 \neq i_2 \end{cases} \quad (1)$$

That is, the cross-correlation of two MPCs is either zero or one, depending on whether they are in the same group or not, respectively. Based on this property, one MPC, say, the pth MPC, in every group is reserved as a reference code, and the remaining codes are used as signature codes to transmit data to $(p^2 - p)$ users, respectively. In the $\boldsymbol{C}_{i,j}$ receiver, the reference code belongs to the ith group is used to estimate the MUI. For example, assuming that four bit-1s are transmitted to $\boldsymbol{C}_{1,1}$, $\boldsymbol{C}_{2,1}$, $\boldsymbol{C}_{2,2}$ and $\boldsymbol{C}_{3,2}$ receivers, respectively, and one bit-0 which is transmitted by zero power is transmitted to the $\boldsymbol{C}_{1,2}$ receiver, the $\boldsymbol{C}_{2,1}$ receiver will receive two chip-power MUI. Since the MUI to $\boldsymbol{C}_{2,1}$ is the same as that to $\boldsymbol{C}_{2,3}$, the $\boldsymbol{C}_{2,1}$ receiver can use the reference code $\boldsymbol{C}_{2,3}$ to estimate the MUI.

For OOK systems, the interference estimator has to estimate the MUI for every bit since the MUI varies from bit to bit. Consequently, the data rate in such systems is severely limited by the electronic processing time in estimating MUI and tuning the threshold device. To avoid the varying MUI, the balanced encoder had been used for optical code-division multiplexing (OCDM) systems [20, 21]. Based on the balanced encoding, the MUI contributed by any user is constant. For OCDM systems with fixed number of simultaneous users, the MUI is constant and no MUI estimator is needed. However, for OCDMA systems, the number of simultaneous users is no longer fixed. To overcome this problem, an OCDMA system that maintains the MUI constant during a frame is proposed. In the proposed system, the MUI estimation is needed at the beginning of each frame only. Moreover, since the parallel processes in estimating the MUI and detecting data are no longer needed, it is possible to simplify the hardware of the receiver. Based on the performance analysis, the numerical results show that the proposed OCDMA system has lower bit error rate (BER) than the original OOK–OCDMA system since it uses full power in estimating the MUI and in detecting data. The numerical results also show that the BER is even lower if more training bits are used to estimate the MUI.

In the remainder of this paper, the structures of the encoder and decoder, the slot timing, and the frame format for the proposed OCDMA system are introduced in Section 2. The performance analysis is carried out in Section 3, and the numerical results are shown in Section 4. Finally, conclusions are given in Section 5.

Table 1 Modified prime codes for $p = 3$

Group	MPCs
1	$\boldsymbol{C}_{1,1} = 100\ 100\ 100$
	$\boldsymbol{C}_{1,2} = 010\ 010\ 010$
	$\boldsymbol{C}_{1,3} = 001\ 001\ 001$
2	$\boldsymbol{C}_{2,1} = 100\ 010\ 001$
	$\boldsymbol{C}_{2,2} = 010\ 001\ 100$
	$\boldsymbol{C}_{2,3} = 001\ 100\ 010$
3	$\boldsymbol{C}_{3,1} = 100\ 001\ 010$
	$\boldsymbol{C}_{3,2} = 010\ 100\ 001$
	$\boldsymbol{C}_{3,3} = 001\ 010\ 100$

2 System description

The OCDMA system considered in this paper is a star network with a central star coupler. Each node uses a specific code to receive data. In order to have more nodes, the extended MPCs (EMPCs) [22] are used as spreading codes. Other spreading codes that have constant cross-correlation, for example, the perfect difference codes [8] and Manchester coded Walsh codes [21], can be implemented in a similar way. The EMPCs have the same correlation properties as MPCs while they have one more external group of p codes for each prime number p. That is, there are $(p^2 + p)$ EMPCs for each p. For example, the total EMPCs for $p = 3$ are shown in Table 2.

Table 2 Extended modified prime codes for $p = 3$

Group	EMPCs
1	$\boldsymbol{C}_{1,1} = 100\ 100\ 100$
	$\boldsymbol{C}_{1,2} = 010\ 010\ 010$
	$\boldsymbol{C}_{1,3} = 001\ 001\ 001$
2	$\boldsymbol{C}_{2,1} = 100\ 010\ 001$
	$\boldsymbol{C}_{2,2} = 010\ 001\ 100$
	$\boldsymbol{C}_{2,3} = 001\ 100\ 010$
3	$\boldsymbol{C}_{3,1} = 100\ 001\ 010$
	$\boldsymbol{C}_{3,2} = 010\ 100\ 001$
	$\boldsymbol{C}_{3,3} = 001\ 010\ 100$
4	$\boldsymbol{C}_{4,1} = 111\ 000\ 000$
	$\boldsymbol{C}_{4,2} = 000\ 111\ 000$
	$\boldsymbol{C}_{4,3} = 000\ 000\ 111$

doi: 10.1049/iet-opt.2008.0021

The encoder, decoder, slot timing and frame format of the proposed system are described in the following subsections.

2.1 Encoder

The structure of the balance encoder is shown in Fig. 2. The data bit $b = 0$ and $b = 1$ are encoded by the upper branch and lower branch, respectively. The optical encoder uses tunable delay lines, which are widely implemented in recent two-dimensional OCDMA systems [23, 24], to encode the transmitting bit into destination code sequence. In each group of EMPCs, $(p-1)$ EMPCs are allotted to transmit bit-1s to $(p-1)$ specific receivers, respectively, and the remaining EMPC is reserved as the common code to transmit bit-0s to the $(p-1)$ receivers. Therefore there can be up to (p^2-1) nodes in the system. As long as the number of simultaneous users is fixed, the MUI at each receiver maintains fixed, no matter what contents the interferers are transmitting. This is a key difference between the balanced encoding systems and OOK systems since the MUI in OOK systems varies with the number of interferers who are transmitting bit-1s.

2.2 Decoder

The structure of the proposed decoder is shown in Fig. 3, which is basically an OOK decoder instead of a balanced decoder. Let I be the number of interferers. The received power at the output of correlator can be expressed as

$$P_{CR} = \begin{cases} (p+I)P_R/p, & \text{for } b=1 \\ IP_R/p & \text{for } b=0 \end{cases} \quad (2)$$

where P_R is the received chip-power and the optical correlator is assumed to be the delay-line correlator [2, 25]. Based on the slot timing and frame format described in the following subsections, all of the beginning bits of each frame are 0s; hence, the decoder can obtain the interference power (IP_R/p). Therefore, at the beginning of each frame, the decoder can estimate the MUI and determine the threshold θ. To reduce the variance of the estimated θ, the decoder uses W training bits to obtain an averaged θ. The rule in determining θ will be discussed in the next section. After the estimation, the receiver detects the received data. Since the MUI estimation is carried out at the beginning of each frame only, the data rate of the system is no longer limited by the electronic processing time needed in the MUI estimation. Moreover, since the MUI estimation and data detection are now performed sequentially, the hardware of the new decoder is much simpler than the one shown in Fig. 1.

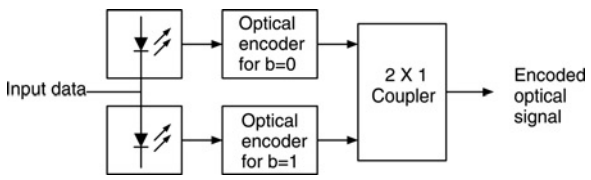

Figure 2 *Structure of OCDMA balance encoder*

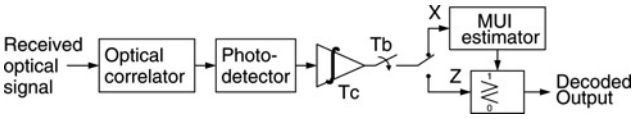

Figure 3 *Serial structure of OCDMA decoder with interference estimator*

2.3 Slot timing

In the proposed OCDMA system, each node in the system is assumed synchronised to a common clock. The control node periodically broadcasts a clock beacon and each node adjusts its clock to maintain the synchronisation. In the timing diagram shown in Fig. 4, three frames whose destinations are, respectively, U_1, U_4 and U_5 are received at some receiver. Every frame is transmitted at the same time t_T. In order to ensure that every receiver has received all of the simultaneous frames, the receiver begins to estimate the MUI at $t_E = t_T + T_{MD}$, where T_{MD} is the maximal possible propagation delay. In the duration from t_E to t_D, the receiver uses W training bits to estimate the MUI and then tunes the threshold θ. The duration $(t_D - t_E)$ is determined according to W and the electronic processing time in determining θ. After that, from t_D to t_N, the received signal is switched to the threshold device to determine the received bits.

2.4 Frame format

As shown in Fig. 4, each frame consists of the following three fields.

(1) *Preamble field*: The preamble consists of all zero bits. The length of the preamble must ensure that every receiver can obtain the bit-0s from all of the transmitted frames to estimate the MUI during the training period from t_E to t_D. Let T_{PM} denote the length of the preamble in seconds. We have

$$T_{PM} \geq t_D - t_T \quad (3)$$

(2) *Data field*: The data field consists of header bits and the payload. Since all preamble bits are zeros, the first bit of the header must be 1 to declare the beginning of the data field. To ensure that the last bit can reach the receiver before t_N, we have

$$T_{DTA} \leq t_N - t_E - T_{PM} \quad (4)$$

where T_{DTA} is the length of the data field in seconds.

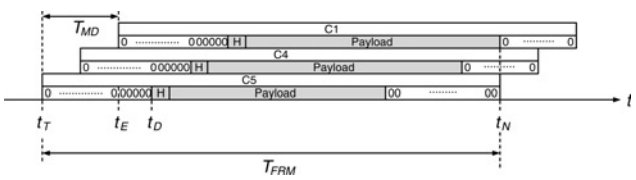

Figure 4 *Received frames at some receiver*

(3) *Pad field*: In order to maintain the constant MUI in the detecting period, the length of each frame should be padded to $(t_N - t_T)$ seconds. Let T_{PD} denote the length of the pad field. We have

$$T_{PD} = t_N - t_T - T_{PM} - T_{DTA} \tag{5}$$

Inserting (4) into (5), we have

$$T_{PD} \geq t_E - t_T = T_{MD} \tag{6}$$

Under the frame format, the throughput becomes $[R{\cdot}T_{DTA}/(T_{PM} + T_{DTA} + T_{PD})]$, where R is the data rate. Although the preamble and pad fields reduce the throughput, the final throughput is still high because R is increased because of the reduction of electronic processing time for each bit.

3 Performance analysis

Assume that there are $(p^2 - 1)$ nodes. Let N be the number of simultaneous users and I be the number of interferers who contribute MUI. The probability mass function of I can be written as

$$p_I(i) = \begin{cases} \dfrac{\binom{p^2-p}{i}\binom{p-2}{N-i-1}}{\binom{p^2-2}{N-1}}, & \text{for } i \in \{i_{min}, i_{min}+1, \ldots, i_{max}\} \\ 0, & \text{otherwise} \end{cases} \tag{7}$$

where $i_{min} = \max\{0, N - p + 1\}$ and $i_{max} = \min\{p^2 - p, N - 1\}$.

Let the input of the MUI estimator be X and assume that the photo-detector is an avalanche photodiode (APD). Given $I = i$, the conditional probability density function (pdf) of X using the Gaussian model including APD noise and thermal noise can be written as follows [26, 27]

$$f_X(x|I=i) = \frac{1}{\sqrt{2\pi\sigma^2_{X|I=i}}} \exp\left(-\frac{(x-\mu_{X|I=i})^2}{2\sigma^2_{X|I=i}}\right) \tag{8}$$

where

$$\mu_{X|I=i} = GT_c(i\lambda_s + I_b/e) + T_cI_s/e \tag{9}$$

$$\sigma^2_{X|I=i} = G^2F_eT_c(i\lambda_s + I_b/e) + T_cI_s/e + \sigma^2_{th} \tag{10}$$

In (9) and (10)

$$\lambda_s = \eta P_R/hfp \tag{11}$$

Table 3 Link parameters

Name	Symbol	Value
wavelength	λ	1300 nm
APD quantum efficiency	η	0.6
APD gain	G	100
APD bulk leakage current	I_b	0.1 nA
APD surface leakage current	I_s	10 nA
APD effective ionisation ratio	k_{eff}	0.02
chip duration	T_c	0.1 ns
receiver noise temperature	T_r	300 K
receiver load resistance	R_L	1000 Ω

The definitions of the symbols G, T_c, I_b, I_s and η are given in Table 3. The symbols h, f, e and F_e are, respectively, the Planck's constant, the frequency of light source, an electron charge equal to 1.6×10^{-19} Coulomb, and the excess noise factor expressed by

$$F_e = k_{eff}G + (2 - 1/G)(1 - k_{eff}) \tag{12}$$

where k_{eff} is the APD effective ionization ratio. The σ^2_{th} in (10) is the variance of thermal noise given by

$$\sigma^2_{th} = 2k_BT_rT_c/(e^2R_L) \tag{13}$$

where k_B is the Boltzmann's constant, T_r is the receiver noise temperature and R_L is the load resistance.

Similarly, the conditional pdf of Z, which is the input of the threshold device, can be written as

$$f_Z(z|I=i) = \frac{1}{\sqrt{2\pi\sigma^2_{Z|I=i}}} \exp\left(-\frac{(z-\mu_{Z|I=i})^2}{2\sigma^2_{Z|I=i}}\right) \tag{14}$$

where ((15) and (16))

Given $I = i$, the error probability can be computed as follows

$$\begin{aligned} P_{e|I=i} &= \Pr\{b=1\} \cdot \Pr\{Z < \theta | b=1, I=i\} \\ &\quad + \Pr\{b=0\} \cdot \Pr\{Z > \theta | b=0, I=i\} \\ &= \frac{1}{4}\left[\operatorname{erfc}\left(\frac{\theta-\mu_0}{\sqrt{2\sigma_0^2}}\right) + \operatorname{erfc}\left(\frac{\mu_1-\theta}{\sqrt{2\sigma_1^2}}\right)\right] \end{aligned} \tag{17}$$

$$\mu_{Z|I=i} = \begin{cases} \mu_1 = GT_c[(i+p)\lambda_s + I_b/e] + T_cI_s/e, & \text{for } b=1 \\ \mu_0 = GT_c(i\lambda_s + I_b/e) + T_cI_s/e, & \text{for } b=0 \end{cases} \tag{15}$$

$$\sigma^2_{Z|I=i} = \begin{cases} \sigma_1^2 = G^2F_eT_c[(i+p)\lambda_s + I_b/e] + T_cI_s/e + \sigma^2_{th}, & \text{for } b=1 \\ \sigma_0^2 = G^2F_eT_c(i\lambda_s + I_b/e) + T_cI_s/e + \sigma^2_{th}, & \text{for } b=0 \end{cases} \tag{16}$$

doi: 10.1049/iet-opt.2008.0021

where erfc(·) is the complementary error function defined as

$$\mathrm{erfc}(x) = \frac{2}{\sqrt{\pi}} \int_x^\infty \exp(-t^2)\,\mathrm{d}t \tag{18}$$

To minimise the BER, the optimal value of θ, which is a function of i, can be derived from $\partial P_{e|I=i}/\partial\theta = 0$ [16]

$$\theta(i) = \frac{b + \sqrt{b^2 - ac}}{a} \tag{19}$$

where

$$a = \sigma_1^2 - \sigma_0^2$$
$$b = \sigma_1^2\mu_0 - \sigma_0^2\mu_1$$
$$c = \sigma_1^2\mu_0^2 - \sigma_0^2\mu_1^2 + \sigma_0^2\sigma_1^2 \cdot \ln\left(\frac{\sigma_0^2}{\sigma_1^2}\right)$$

If the receiver knew the exact value of I, the optimal threshold could be determined by (19), and the optimal BER could be computed by the following equation

$$P_{\mathrm{e,opt}} = \sum_{i=i_{\min}}^{i_{\max}} P_{e|I=i} p_I(i) \tag{20}$$

However, since the exact value of I may be different for different frames, the value of I and hence the threshold θ should be estimated in the estimation duration from t_{E} to t_{D}. In the following, two methods in estimating the threshold are introduced.

3.1 Non-linear estimation

Based on (9), the unbiased estimation of I can be obtained by

$$\tilde{I}_{W=1} = \left(X - \frac{T_{\mathrm{c}}(GI_{\mathrm{b}} + I_{\mathrm{s}})}{e}\right) / GT_{\mathrm{c}}\lambda_{\mathrm{s}} \tag{21}$$

where the suffix $W = 1$ means that only one preamble bit is used.

The pdf of $\tilde{I}_{W=1}$ is Gaussian with the following mean and variance

$$\mu_{\tilde{I}_{W=1}} = I \tag{22}$$

$$\sigma^2_{\tilde{I}_{W=1}} = \frac{\sigma_X^2}{(GT_{\mathrm{c}}\lambda_{\mathrm{s}})^2} \tag{23}$$

For W preamble bits used, the mean of $\tilde{I}_W$ would be the same as (22) while the variance would become

$$\sigma^2_{\tilde{I}_W} = \frac{\sigma_X^2}{W(GT_{\mathrm{c}}\lambda_{\mathrm{s}})^2} \tag{24}$$

which means that the estimation of interference is more accurate for larger W.

Given $\tilde{I}_W = \tilde{i}$, the threshold can be estimated as

$$\tilde{\theta}_{\mathrm{NL}}(\tilde{i}) = \frac{\tilde{b} + \sqrt{\tilde{b}^2 - \tilde{a}\tilde{c}}}{\tilde{a}} \tag{25}$$

where

$$\tilde{a} = \tilde{\sigma}_1^2 - \tilde{\sigma}_0^2$$
$$\tilde{b} = \tilde{\sigma}_1^2\tilde{\mu}_0 - \tilde{\sigma}_0^2\tilde{\mu}_1$$
$$\tilde{c} = \tilde{\sigma}_1^2\tilde{\mu}_0^2 - \tilde{\sigma}_0^2\tilde{\mu}_1^2 + \tilde{\sigma}_0^2\tilde{\sigma}_1^2 \cdot \ln\left(\frac{\tilde{\sigma}_0^2}{\tilde{\sigma}_1^2}\right)$$

In (25), the estimated parameters are

$$\tilde{\mu}_1 = GT_{\mathrm{c}}[(\tilde{i} + p)\lambda_{\mathrm{s}} + I_{\mathrm{b}}/e] + T_{\mathrm{c}}I_{\mathrm{s}}/e \tag{26}$$

$$\tilde{\mu}_0 = GT_{\mathrm{c}}(\tilde{i}\lambda_{\mathrm{s}} + I_{\mathrm{b}}/e) + T_{\mathrm{c}}I_{\mathrm{s}}/e \tag{27}$$

$$\tilde{\sigma}_1^2 = G^2F_{\mathrm{e}}T_{\mathrm{c}}[(\tilde{i} + p)\lambda_{\mathrm{s}} + I_{\mathrm{b}}/e] + T_{\mathrm{c}}I_{\mathrm{s}}/e + \sigma_{\mathrm{th}}^2 \tag{28}$$

$$\tilde{\sigma}_0^2 = G^2F_{\mathrm{e}}T_{\mathrm{c}}(\tilde{i}\lambda_{\mathrm{s}} + I_{\mathrm{b}}/e) + T_{\mathrm{c}}I_{\mathrm{s}}/e + \sigma_{\mathrm{th}}^2 \tag{29}$$

Finally, the BER becomes (30)

where $f_{\tilde{I}_W}(\tilde{i})$ is the pdf of $\tilde{I}_W$ under the condition $I = i$.

3.2 Linear estimation

In practice, the non-linear estimation of the threshold is somewhat complex. To reduce the complexity, consider the following threshold

$$\begin{aligned}\theta_{\mathrm{L}} &= \mu_0 + \alpha(\mu_1 - \mu_0) \\ &= \mu_0 + \alpha GT_{\mathrm{c}}\lambda_{\mathrm{s}}p\end{aligned} \tag{31}$$

where α is a predetermined constant. Based on this threshold, the BER can be expressed as (32)

Since $i_{\min}$ and $i_{\max}$ are functions of N, the optimal value of α that minimises the BER is also a function of N. Based on

$$P_{\mathrm{e,NL}} = \sum_{i=i_{\min}}^{i_{\max}} p_I(i) \cdot \frac{1}{4} \int_{-\infty}^{\infty} \left[\mathrm{erfc}\left(\frac{\tilde{\theta}(\tilde{i}) - \mu_0}{\sqrt{2\sigma_0^2}}\right) + \mathrm{erfc}\left(\frac{\mu_1 - \tilde{\theta}(\tilde{i})}{\sqrt{2\sigma_1^2}}\right)\right] f_{\tilde{I}_W}(\tilde{i})\,\mathrm{d}\tilde{i} \tag{30}$$

$$P_{\mathrm{e,L}} = \sum_{i=i_{\min}}^{i_{\max}} p_I(i) \frac{1}{4} \left[\mathrm{erfc}\left(\frac{\alpha(\mu_1 - \mu_0)}{\sqrt{2\sigma_0^2}}\right) + \mathrm{erfc}\left(\frac{(1-\alpha)(\mu_1 - \mu_0)}{\sqrt{2\sigma_1^2}}\right)\right] \tag{32}$$

the criterion that minimises the fully loaded BER, we choose the following sub-optimal value of α that minimises the BER for $N = p^2 - 1$ (see (33))

where the parameters under full load are

$$\mu_{1,\mathrm{FL}} = GT_c(p^2\lambda_s + I_b/e) + T_cI_s/e \tag{34}$$

$$\mu_{0,\mathrm{FL}} = GT_c[(p^2 - p)\lambda_s + I_b/e] + T_cI_s/e \tag{35}$$

$$\sigma^2_{1,\mathrm{FL}} = G^2F_eT_c(p^2\lambda_s + I_b/e) + T_cI_s/e + \sigma^2_{\mathrm{th}} \tag{36}$$

$$\sigma^2_{0,\mathrm{FL}} = G^2F_eT_c[(p^2 - p)\lambda_s + I_b/e] + T_cI_s/e + \sigma^2_{\mathrm{th}} \tag{37}$$

In practical situation, the only parameter in (31) to be estimated is μ_0. Let X_W be the averaged value of X during W training bits. The pdf of X_W is Gaussian with the following mean and variance

$$\mu_{X_W} = \mu_0 \tag{38}$$

$$\sigma^2_{X_W} = \sigma^2_0/W \tag{39}$$

Therefore we can use X_W as the unbiased estimation of μ_0, and the estimated threshold becomes

$$\tilde{\theta}_{\mathrm{L}} = X_W + \alpha GT_c\lambda_s p \tag{40}$$

The pdf of $\tilde{\theta}_{\mathrm{L}}$ is also Gaussian with the following mean and variance

$$\mu_{\tilde{\theta}_{\mathrm{L}}} = \mu_0 + \alpha GT_c\lambda_s p \tag{41}$$

$$\sigma^2_{\tilde{\theta}_{\mathrm{L}}} = \sigma^2_0/W \tag{42}$$

Let $Y = Z - \tilde{\theta}_{\mathrm{L}}$. We have the following Gaussian mean and variance

$$\mu_Y = \begin{cases} \mu_{Y_1} = (1-\alpha)GT_c\lambda_s p, & \text{for } b = 1 \\ \mu_{Y_0} = -\alpha GT_c\lambda_s p, & \text{for } b = 0 \end{cases} \tag{43}$$

$$\sigma^2_Y = \begin{cases} \sigma^2_{Y_1} = \sigma^2_1 + \sigma^2_0/W, & \text{for } b = 1 \\ \sigma^2_{Y_0} = \sigma^2_0 + \sigma^2_0/W, & \text{for } b = 0 \end{cases} \tag{44}$$

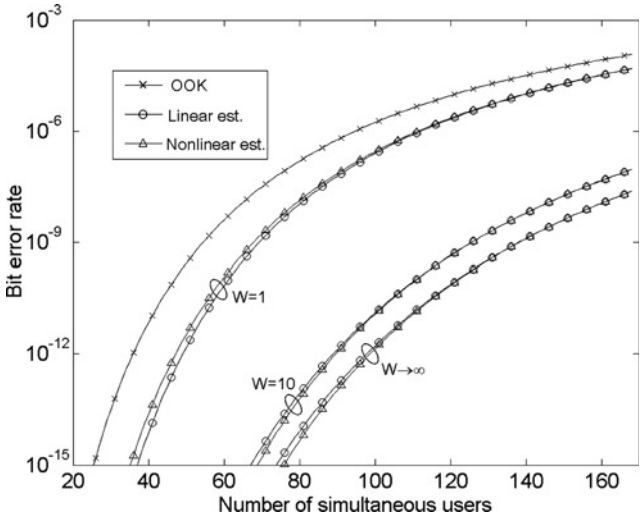

Figure 5 *Bit error rates of constant interference OCDMA systems and OOK–OCDMA system ($p = 13$, $P_R = 15$ μW)*

Finally, the BER can be computed as

$$\begin{aligned} P_{\mathrm{e,L}} &= \sum_{i=i_{\min}}^{i_{\max}} p_I(i) \cdot [\Pr\{b=1\} \cdot \Pr\{Y < 0 | b = 1, I = i\} \\ &\quad + \Pr\{b=0\} \cdot \Pr\{Y > 0 | b = 0, I = i\}] \\ &= \sum_{i=i_{\min}}^{i_{\max}} p_I(i) \cdot \frac{1}{4}\left[\mathrm{erfc}\left(\frac{\mu_{Y_1}}{\sqrt{2\sigma^2_{Y_1}}}\right) + \mathrm{erfc}\left(\frac{-\mu_{Y_0}}{\sqrt{2\sigma^2_{Y_0}}}\right)\right] \end{aligned} \tag{45}$$

4 Numerical results

In this section, we calculate the numerical results according to the parameters listed in Table 3. The BERs of proposed OCDMA systems using non-linear and linear estimated thresholds for $p = 13$ and $P_R = 15$ μW are shown in Fig. 5. Under the same parameters, the BER of the OOK–OCDMA system with the receiver shown in Fig. 1 using threshold $\tilde{\theta}_{\mathrm{OOK}} = X + 0.45GT_c\lambda_s p$, which is suggested in [19], is also shown in Fig. 5. By comparing the BERs of the OOK system and those of the proposed systems with $W = 1$, it could be found that balanced encoding systems have lower BERs, though the average MUI in the OOK system is smaller. The reason for this phenomenon is that the balanced encoding system can serially use full received power to estimate the MUI and to detect data, whereas the OOK system has to split the received power to the parallel estimator and detector. Since the linear estimating system is designed to obtain the minimal BER under full load, it could be found that the

$$\alpha = \frac{-\sigma^2_{0,\mathrm{FL}} + \sqrt{\sigma^4_{0,\mathrm{FL}} + (\sigma^2_{1,\mathrm{FL}} - \sigma^2_{0,\mathrm{FL}})\sigma^2_{0,\mathrm{FL}}\sigma^2_{1,\mathrm{FL}} \ln(\sigma^2_{1,\mathrm{FL}}/\sigma^2_{0,\mathrm{FL}})/(\mu_{1,\mathrm{FL}} - \mu_{0,\mathrm{FL}})^2}}{(\sigma^2_{1,\mathrm{FL}} - \sigma^2_{0,\mathrm{FL}})} \tag{33}$$

doi: 10.1049/iet-opt.2008.0021

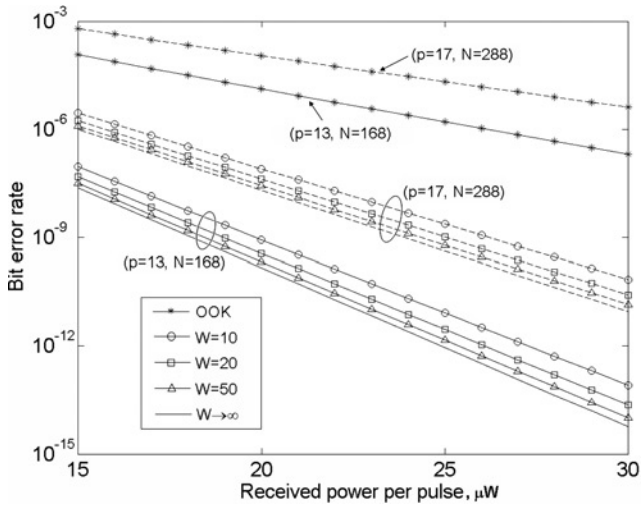

Figure 6 *Fully loaded BER against received power for constant interference OCDMA systems and OOK–OCDMA system ($p = 13$ and $p = 17$)*

difference between the BERs of the non-linear and linear estimating systems decreases with the increased N. As the number of training bits W increases, the BER of the proposed system decreases apparently. For $W = 10$, the proposed system can afford 125 simultaneous users under the constrain BER $< 10^{-9}$.

Under full load, the BERs against received power P_R of the proposed system with linear estimator for $p = 13$ and $p = 17$ are shown in Fig. 6 for various W. Obviously, the BERs of balanced encoding OCDMA systems are much smaller than that of the OOK system. As long as the power and the number of training bits are large enough, the BER of the proposed system can reach an acceptable range even in full loaded case.

5 Conclusion

In this paper, the balanced encoding scheme is used instead of OOK. The slot timing and the frame format to maintain constant MUI in a frame are discussed. The receiver in the proposed OCDMA system needs only to estimate the MUI at the beginning of a frame instead of estimating bit by bit; therefore, the data rate is no longer severely limited by the electronic processing time in estimating the MUI and tuning the threshold device. The maximal number of nodes in the proposed system is the same as that in the OOK system with interference estimator. Although the balance encoder is more complex than the OOK encoder, the receiver in the proposed system is simpler. In the receiver, two kinds of threshold estimator are introduced. Numerical results show that the proposed OCDMA systems have smaller BER than the OOK system. The BER of the proposed system can be further reduced by slightly increasing the number of training bits. Numerical results also show that the system with linear estimator, which is much simpler than the non-linear estimator, has good performance, especially when the number of simultaneous users is large. As the number of training bits and signal power are large enough, the system has acceptable BER for many simultaneous users.

6 References

[1] PRUCNAL P.R., SANTORO M.A., FAN T.R.: 'Spread spectrum fiber-optic local area network using optical processing', *J. Lightwave Technol.*, 1986, **4**, (5), pp. 547–554

[2] SALEHI J.A.: 'Code division multiple-access techniques in optical fiber networks – Part I: Fundamental principles', *IEEE Trans. Commun.*, 1989, **37**, (8), pp. 824–833

[3] RATNAM J.: 'Optical CDMA in broadband communication – scope and applications', *J. Opt. Commun.*, 2002, **23**, (1), pp. 11–21

[4] STOK A., SARGENT E.H.: 'The role of the optical CDMA in access networks', *IEEE Commun. Mag.*, 2002, **40**, (8), pp. 83–87

[5] CHUNG F.R.K., SALEHI J.A., WEI V.K.: 'Optical orthogonal codes: Design, analysis, and applications', *IEEE Trans. Inf.. Theory*, 1989, **35**, (3), pp. 595–604

[6] KWONG W.C., PERRIER P.A., PRUCNAL P.R.: 'Performance comparison of asynchronous and synchronous code-division multiple-access techniques for fiber-optic local area networks', *IEEE Trans. Commun.*, 1991, **39**, (11), pp. 1625–1634

[7] ZHANG J.G.: 'Design of a special family of optical CDMA address codes for fully asynchronous data communications', *IEEE Trans. Commun.*, 1999, **47**, (7), pp. 967–973

[8] WENG C.-S., WU J.: 'Perfect difference codes for synchronous fiber-optic CDMA communication systems', *J. Lightwave Technol.*, 2001, **19**, (2), pp. 186–194

[9] WENG C.-S., WU J.: 'Optical orthogonal codes with nonideal cross correlation', *J. Lightwave Technol.*, 2001, **19**, (12), pp. 1856–1863

[10] PRUCNAL P.R., SANTORO M.A., SEHGAL S.K.: 'Ultrafast all-optical synchronous multiple access fiber networks', *IEEE J. Sel. Areas Commun.*, 1986, **4**, (9), pp. 1484–1492

[11] KWONG W.C., PRUCNAL P.R.: 'Synchronous CDMA demonstration for fiber-optic networks with optical processing', *Electron. Lett.*, 1990, **26**, (24), pp. 1990–1992

[12] SALEHI J.A., BRACKETT C.A.: 'Code division multiple-access techniques in optical fiber networks – Part II: Systems

performance analysis', *IEEE Trans. Commun.*, 1989, **37**, (8), pp. 834–842

[13] OHTRSKI T., SATO K., SASASE I., MORI S.: 'Direct-detection optical synchronous CDMA systems with double optical hard-limiters using modified prime sequence codes', *J. Sel. Areas Commun.*, 1996, **14**, (9), pp. 1879–1887

[14] LIN C.-L., WU J.: 'Channel interference reduction using random Manchester codes for both synchronous and asynchronous fiber-optic CDMA systems', *J. Lightwave Technol.*, 2000, **18**, (1), pp. 26–33

[15] LIN C.-L., WU J.: 'A synchronous fiber-optic CDMA system using adaptive optical hardlimiter', *J. Lightwave Technol.*, 1998, **16**, (8), pp. 1393–1403

[16] JAU L.-L., LEE Y.-H.: 'Synchronous optical-CDMA systems using tunable hard limiters', *J. Opt. Commun.*, 2003, **24**, (6), pp. 217–222

[17] WU J.-H., WU J., TSAI C.-N.: 'Synchronous fiber-optic code division multiple access networks with error codes', *Electron. Lett.*, 1992, **28**, (23), pp. 2118–2120

[18] KAMAKURA K., SASASE I.: 'A new modulation scheme using asymmetric error-correcting codes embedded in optical orthogonal codes for optical CDMA', *J. Lightwave Technol.*, 2001, **19**, (12), pp. 1839–1850

[19] SHALABY H.M.H.: 'Synchronous fiber-optical CDMA systems with interference estimators', *J. Lightwave Technol.*, 1999, **17**, (11), pp. 2268–2275

[20] JAU L.-L., LEE Y.-H.: 'Optical code-division multiplexing systems using common zero codes', *Microw. Opt. Technol. Lett.*, 2003, **39**, (2), pp. 165–167

[21] JAU L.-L., LEE Y.-H.: 'Optical code-division multiplexing systems using Manchester coded Walsh codes', *IEE Proc. Optoelectron.*, 2004, **151**, (2), pp. 81–86

[22] JAU L.-L., LEE Y.-H.: 'Optical code-division multiplexing systems using extended prime codes with reused zero codes', *J. Opt. Commun.*, 2006, **27**, (3), pp. 179–183

[23] GLESK I., PRUCNAL P.R., ANDONOVIC I.: 'Incoherent ultrafast OCDMA receiver design with 2 ps all-optical time gate to suppress multiple-access interference', *IEEE J. Sel. Top. Quantum Electron.*, 2008, **14**, (3), pp. 861–867

[24] WILLNER A.E., SAGHARI P., ARBAB V.R.: 'Advanced techniques to increase the number of users and bit rate in OCDMA networks', *IEEE J. Sel. Top. Quantum Electron.*, 2007, **13**, (5), pp. 1403–1414

[25] ZAHEDI S., SALEHI J.A.: 'Analytical comparison of various fiber-optic CDMA receiver structures', *J. Lightwave Technol.*, 2000, **18**, (12), pp. 1718–1727

[26] ABSHIRE J.B.: 'Performance of OOK and lower-order PPM modulations in optical communications when using APD-based receivers', *IEEE Trans. Commun.*, 1984, **32**, (10), pp. 1140–1143

[27] KWON H.M.: 'Optical orthogonal code-division multiple-access system – part I: APD noise and thermal noise', *IEEE Trans. Commun.*, 1994, **42**, (7), pp. 2470–2479

doi: 10.1049/iet-opt.2008.0021